

Dynamical correlations in a Hubbard chain with resonating-valence-bond ground state

Andreas Giesekus

Institut für Physik, Universität Dortmund

D-44221 Dortmund

Germany

Abstract

Dynamical correlation functions for temperature $T = 0$ are calculated for a Hubbard chain with infinite on-site repulsion. This chain contains three sites per unit cell and has a known resonating-valence-bond ground state for a filling of 2 particles per unit cell. A finite system of 24 sites is studied numerically. The recursion method is applied and results for spectral densities are compared to variationally calculated excited-state eigenvalues. Charge and spin degrees of freedom located at the backbone sites are considered. The spectral densities show dispersionless excitations. The energy spectrum displays a gap indicating an insulating ground state. Spectral functions for the propagation of a single hole in a resonating-valence-bond background are provided and indicate delocalized dispersive hole excitations.

71.27.+a, 75.40.Gb

I. INTRODUCTION

The Hubbard model¹ describes electronic interactions in tight binding systems. Although the model itself is very simple, the access to its mathematical properties turns out to be very difficult. The present work is based on an exactly solvable case of the Hubbard model in the strongly interacting limit ($U = \infty$). For that case it has been possible to construct the ground state and the ground-state energy.² The class of models which are solvable by this method has been generalized by Strack,³ Bares and Lee⁴ and Tasaki.^{5,6}

The ground state of those models exhibits the structure of a resonating-valence-bond (RVB) state.⁵ One-dimensional models of this class³ allowed for the calculation of equal-time correlation functions⁴ using a transfer-matrix technique.

All studies conducted so far have been concerned with equilibrium properties of the ground state. Although the explicit knowledge of a Hamiltonian for the fermionic realization of an RVB-system enables one to study the excitation spectrum and dynamical quantities, no analytical statements about those quantities have been possible up to now.

This paper presents a numerical treatment of excitations in a one-dimensional representative of the class of exactly solvable models introduced in [2]. Dynamical correlation functions are calculated by a recursive algorithm. The resulting spectral properties are corroborated by a variational calculation of excited states and their energies. The method used here allows the calculation of single-hole spectral-functions as well. In principle these spectral functions are related to inverse photoemission spectra.

II. THE MODEL HAMILTONIAN

A linear chain with N unit cells and $3N$ sites is studied. The topology of this chain is illustrated in Fig. 1; it may be interpreted as a chain of connected tetrahedra. The case of infinite on-site repulsion is assumed, which implies that only particle numbers below half-filling exhibit non-trivial dynamics. The ground state can be constructed for particle

densities of two or more per unit cell,² thus the chain must have at least three sites (labeled by indices α, β) per unit cell.

The dimensionless Hamiltonian (the hopping matrix element defines the energy scale only and is set to unity) of the system under investigation is written as:

$$\begin{aligned} H = & P \left\{ - \sum_{i,\sigma} \sum_{\alpha \neq \beta} c_{i,\alpha,\sigma}^\dagger c_{i,\beta,\sigma} \right. \\ & - \sum_{i,\sigma} \sum_{\alpha} (c_{i-1,1,\sigma}^\dagger c_{i,\alpha,\sigma} + h.c.) \\ & \left. - 2 \sum_{i,\sigma} n_{i,1,\sigma} \right\} P, \end{aligned} \quad (1)$$

where $c_{i,\alpha,\sigma}^\dagger$ creates an electron in the unit cell $i \in \{1, \dots, N\}$ at site $\alpha \in \{1, 2, 3\}$ with spin $\sigma \in \{\uparrow, \downarrow\}$. The operators $n_{i,\alpha,\sigma}$ denote the corresponding occupation number operators. Periodic boundary conditions are assumed. As mentioned above, an infinitely strong on-site interaction is included by projecting all states onto the subspace without doubly occupied sites:

$$P = \prod_{i,\alpha} (1 - n_{i,\alpha,\uparrow} n_{i,\alpha,\downarrow}) \quad (2)$$

The last term in (1) is a local field that lowers the energy of the connection sites $\alpha = 1$. It ensures an almost uniform distribution of particles in the chain: The ground-state probability for finding an electron with spin σ on a site with $\alpha = 1$ ($\alpha = 2, 3$) in a particular unit cell has been calculated as 0.3612 (0.3194) for a chain with six unit cells.

III. THE GROUND STATE

The ground state is derived by the same arguments as presented in [2]. Consider a linear combination of the creation operators $c_{i,\alpha,\sigma}^\dagger$:

$$\Psi_{i,\sigma}^\dagger := c_{i-1,1,\sigma}^\dagger + \sum_{\alpha} c_{i,\alpha,\sigma}^\dagger \quad (3)$$

By some elementary algebra, the Hamiltonian (1) can be exactly converted to the following form

$$H = P \{2N_e - 8N\} + \sum_{i,\sigma} \Psi_{i,\sigma} P \Psi_{i,\sigma}^\dagger, \quad (4)$$

where N_e denotes the total electron number operator of the system. The Hamiltonian now consists of a trivial term $P(2N_e - 8N)$ and a remainder. This remainder is positive semidefinite, therefore the ground-state energy is bounded from below by $E_0 \geq 2N_e - 8N$, where N_e denotes the eigenvalue of the electron-number operator N_e . Additionally, an upper bound can be derived: Any expectation value of the Hamiltonian (4) is greater than or equal to the ground-state energy. The operator identity

$$P \Psi_{i,\sigma}^\dagger P \Psi_{i,\sigma}^\dagger \equiv 0 \quad (5)$$

allows to construct states which are eigenstates of the remainder operator $\sum_{i,\sigma} \Psi_{i,\sigma} P \Psi_{i,\sigma}^\dagger$ with eigenvalue zero. Any state

$$|\Phi_0\rangle := P \prod_i \Psi_{i,\uparrow}^\dagger \Psi_{i,\downarrow}^\dagger |\chi\rangle \quad (6)$$

has this property. If $|\chi\rangle$ denotes the vacuum state $|0\rangle$, $|\Phi_0\rangle$ is simply a Gutzwiller-projected Slater determinant with two electronic orbitals in each unit cell.

The solvability of the model is based on Eq. (5), a relation that holds because a local summation over fermionic operators vanishes due to their phase and the topology of the unit cell. This local property will be visible in the spectral results of the ground-state dynamics studied below.

It is mentioned in passing that the norm of the states (6) is not zero, a fact that is not trivial and has been proven.² For any finite system, the ground state with $|\chi\rangle = |0\rangle$ is non-degenerate. This has been conjectured by Brandt and Giesekus² and proven by Tasaki⁶ (and Bares and Lee⁴ for a special case), whereas a ground state with more than $2N$ particles is obviously degenerate.

Tasaki⁵ pointed out that the ground state is generated by linear combinations of creation operators that contain only terms like $c_{i,\alpha,\uparrow}^\dagger c_{j,\beta,\downarrow}^\dagger - c_{i,\alpha,\downarrow}^\dagger c_{j,\beta,\uparrow}^\dagger$. These terms create spin singlets on bonds connecting sites i, α and j, β . Linear combinations with this structure are often called (short range) resonating valence-bond (RVB) states.⁷

IV. SYMMETRIES

For a numerical study of the linear chain it is essential to take advantage of symmetries. They allow to represent the states in terms of a significantly smaller basis set, because only one configuration need be stored as a representative of all states that may be generated from it by symmetry operations.

A. Site interchange

The Hamiltonian is invariant under interchange of sites $\alpha = 2$ and $\alpha = 3$ (see Fig. 1) in every unit cell i . As a consequence there exists an abelian group of 2^N symmetry operations that commute with the Hamilton operator. All 2^N combinations of site interchanges are generated by every single of the 2^N following operators:

$$\mathbf{M}(\{\epsilon_i\}) = \frac{1}{2^N} \prod_{i=1}^N (\mathbf{I} + \epsilon_i \mathbf{M}_i) \quad (7)$$

where \mathbf{M}_i denotes site interchange in unit cell i and \mathbf{I} the unit operator. (The quantity ϵ_i can take the values ± 1 . Note that the product of two such operators vanishes unless they coincide in all signs ϵ_i .)

It is completely equivalent to interpret the *interchange of sites* in terms of an *interchange of particles*, namely those particles that are located on the two participating sites. Then the properties of \mathbf{M}_i acting on fermionic states become obvious immediately: Let the states $|00\rangle$, $|\sigma 0\rangle$, $|0\sigma\rangle$, $|\sigma\sigma'\rangle$ denote empty, singly and doubly occupied bonds. The operator \mathbf{M}_i has the following properties:

- $\mathbf{M}_i|00\rangle = |00\rangle$
- $\mathbf{M}_i|\sigma 0\rangle = |0\sigma\rangle$, $\mathbf{M}_i|0\sigma\rangle = |\sigma 0\rangle$
- $\mathbf{M}_i|\sigma\sigma'\rangle = -|\sigma'\sigma\rangle$.

From these properties, it follows immediately that the operator $\frac{1}{2}(I + M_i)$ not only generates the site interchange, it additionally may be interpreted as a projector onto spin singlets for doubly occupied bonds. The operator $\frac{1}{2}(I - M_i)$ projects onto triplet states.

The symmetry of every eigenstate of the Hamiltonian may be classified according to 2^N different sets of signs $\{\epsilon_i\}$ [see Eq. (7)]. The ground state may be written as

$$|\Phi_0\rangle = \mathbf{M}_s |\tilde{\Phi}_0\rangle. \quad (8)$$

where \mathbf{M}_s (the index s indicates that all $2 - 3$ -bonds are projected on the singlet-subspace) is an abbreviation for $\mathbf{M}(\{\epsilon_i = +1\})$. This is possible, because the ground state consists of singlets only. However, it is important to keep in mind that excited states may not necessarily be written in this way. The state $|\tilde{\Phi}_0\rangle$ requires much less computer memory, because it is only necessary to store one representative basis state for the whole class of about 2^N basis states that are connected by a simple interchange of sites $\alpha = 2, 3$.

B. Translational invariance

The second kind of symmetries that is taken explicitly into account is the translational invariance of the Hamiltonian. Periodic boundary conditions are assumed. Let T_l be the operator that shifts all electrons on the chain l unit cells to the right. Again, fermion states are totally antisymmetric under interchange of particles, hence translation of states (which may be described in terms of particle interchange) may cause a phase. For the case of $l = 1$ (shift by one unit cell) the resulting sign is given by $(-1)^{n(N_e - n)}$, where N_e is the total number of electrons in the system and n the number of electrons in the last unit cell that are transferred to the first unit cell (i. e. moved across the “border”). The operator

$$\mathbf{T}_q = \frac{1}{\sqrt{N}} \sum_{l=1}^N e^{iql} T_l \quad (9)$$

acts as a generator of all translations with symmetry $q = 2\pi m/N$ ($m = 0, \dots, N - 1$). It commutes with the Hamiltonian and with \mathbf{M}_s . (This is not valid for *all* site-interchange symmetries $\mathbf{M}(\{\epsilon_i\})$). The operator \mathbf{T}_q obeys the relation $\mathbf{T}_q \mathbf{T}_{q'} = \delta_{q,q'} \mathbf{T}_q$.

The ground state $|\Phi_0\rangle$ may now be coded by

$$|\Phi_0\rangle = \mathbf{T}_{q=0} \mathbf{M}_s |\bar{\Phi}_0\rangle, \quad (10)$$

where $|\bar{\Phi}_0\rangle$ contains only those basis states that may not be generated from each other by a translation.

It is mentioned in passing that these symmetries lead to selection rules: The scalar product of states can be easily treated if one state has the site-interchange symmetry \mathbf{M}_s : The scalar product of the states $|f\rangle = \mathbf{T}_q \mathbf{M}_s |\bar{f}\rangle$ and $|g\rangle = \mathbf{T}_{q'} \mathbf{M}(\{\epsilon_i\}) |\bar{g}\rangle$ does not vanish if $q = q'$ and all $\epsilon_i = 1$ because \mathbf{M}_s and \mathbf{T}_q commute. This special case is sufficient for the algorithms used below. More general selection rules would have to be derived by group theory because the total group of symmetry operations (site-interchange and translations) is not abelian.

The net storage reduction factor is of the order of $N2^N$ (in fact, the number is slightly smaller, because some basis components may be eigenstates of \mathbf{M}_i [e. g. empty bonds] or \mathbf{T}_l) which reduces the multiplicity of the representative. With these considerations, system sizes of 24 Hubbard sites (eight unit cells) can be treated easily on a workstation.

V. DYNAMICAL CORRELATION FUNCTIONS

This section briefly recalls how dynamical correlation functions at zero temperature are accessible by the recursion method.^{8–12} A detailed discussion can be found in a very recent book by Viswanath and Müller.¹³ Correlation functions of the following type are considered:

$$\tilde{S}(t) = \frac{\langle \Phi_0 | A^\dagger(t) A(0) | \Phi_0 \rangle}{\langle \Phi_0 | A^\dagger(0) A(0) | \Phi_0 \rangle}. \quad (11)$$

The operator A describes the degree of freedom under consideration ($A(t)$ denotes the Heisenberg picture). Below, data are presented for three different A -operators, e. g. $A = S_{q,\alpha=1}^z$, which measures the z -component of the spin located at the connection sites $\alpha = 1$ with a translational symmetry q . Charge degrees of freedom are studied by e. g. $A =$

$\sum_{l,\sigma} \exp\{iql\} n_{l,\alpha,\sigma}$. Because the recursion method is not restricted to hermitean A-operators, the propagation of a single hole may be studied by the operator $A = \sum_l \exp\{iql\} c_{l,\alpha,\sigma}$. Then $\tilde{S}(t)$ [Eq. (11)] becomes a single-particle Green function (for $t > 0$).

All A-operators which are considered here commute with the symmetry generator \mathbf{M}_s of Eq. (8) because they only act on backbone orbitals (degrees of freedom regarding the remaining sites would have to be symmetrized such that they commute with \mathbf{M}_s as well). Therefore the following calculation can be performed without loss of generality in the subspace corresponding to this symmetry. This can be seen immediately by formally expanding the state $\langle \Phi_0 | A^\dagger$ in terms of eigenstates $\langle \Phi_\nu |$ with coefficients α_ν . Then the numerator of Eq. (11) becomes $\sum_\nu \alpha_\nu \exp(-iE_\nu t/\hbar) \langle \Phi_\nu | A | \Phi_0 \rangle$ where E_ν denotes the eigenvalue. The matrix element vanishes if the symmetries of $A | \Phi_0 \rangle$ and $|\Phi_\nu \rangle$ differ.

The method described below requires a positive semidefinite Hamiltonian. Therefore a shifted Hamiltonian $\bar{H} = H - E_0$ is considered where the smallest eigenvalue equals zero. For the hole propagator, the Hamiltonian should be positive semidefinite for particle numbers $N_e = 2N - 1$. Unfortunately the ground-state energy is not known for that case, however, the operator $\bar{H} = H + 4N + 2$ is larger than $\lambda \geq 0$, where λ is the smallest eigenvalue of the non-trivial remainder in (4) for $N_e = 2N - 1$.

Dynamical correlation functions may be derived by an expansion of the state $|\Psi(t)\rangle = A(-t) |\Phi_0\rangle$ which solves the time dependent Schrödinger equation. This state $|\Psi(t)\rangle$ may be expanded in terms of an orthogonal basis¹⁰ $|\Psi(t)\rangle = \sum_k D_k(t) |f_k\rangle$. Then the time evolution of the coefficients $D_k(t)$ is governed by a set of coupled differential equations which may be solved by a Laplace transform.

If this orthogonal basis $|f_k\rangle$ is obtained by the following algorithm (which is closely related to the Lanczos method¹⁴)

$$|f_0\rangle = A |\Phi_0\rangle \quad (12a)$$

$$|f_1\rangle = \bar{H} |f_0\rangle - a_0 |f_0\rangle, \quad (12b)$$

$$|f_2\rangle = \bar{H} |f_1\rangle - a_1 |f_1\rangle - b_1^2 |f_0\rangle, \quad (12c)$$

:

$$|f_{k+1}\rangle = \bar{H}|f_k\rangle - a_k|f_k\rangle - b_k^2|f_{k-1}\rangle, \quad (12d)$$

where

$$a_k = \frac{\langle f_k | \bar{H} | f_k \rangle}{\langle f_k | f_k \rangle} \quad \text{and} \quad b_k^2 = \frac{\langle f_k | f_k \rangle}{\langle f_{k-1} | f_{k-1} \rangle}, \quad (13)$$

the coefficient $D_0(t)$ is identical to $\tilde{S}(t)$ and the series of coefficients a_k , b_k^2 become continued fraction coefficients of the Laplace transform of $\tilde{S}(t)$:

$$\begin{aligned} d_0(\xi) &:= \int_0^\infty dt e^{i\xi t} \tilde{S}(t) \\ &= \frac{i}{\xi - a_0 - \frac{b_1^2}{\xi - a_1 - \frac{b_2^2}{\xi - a_2 \dots}}}. \end{aligned} \quad (14)$$

If all coefficients a_k , b_k^2 are known, the spectral density $S(\omega) = \int_{-\infty}^\infty dt \exp(i\omega t) \tilde{S}(t)$ corresponding to the dynamical correlation function (11) can be recovered by

$$S(\omega) = \lim_{\delta \rightarrow 0} 2 \Re[d_0(\omega + i\delta)], \quad (15)$$

however, only a finite number of continued fraction coefficients can be calculated. Nevertheless, the first few coefficients contain valuable information about the dynamics of the system which will be extracted (as will be discussed in Sec. VI) by more sophisticated means than just cutting off the continued fraction and smearing out by a finite imaginary smear-out parameter δ . A cut-off procedure simply approximates a branch cut by a finite number of isolated singularities, where the number of peaks is determined by the order of the approximation. Additionally, the smear-out parameter δ is often of the same order of magnitude as the hopping matrix element, otherwise reasonably looking results cannot be obtained. In fact, δ must be larger than a typical distance between the isolated singularities in order to produce a sufficient smear-out effect.

Finite Fermi systems have a discrete energy spectrum which only becomes continuous in the thermodynamic limit. Thus a recursive study of a finite Fermi system results in principle

in a finite continued fraction: The recursion will terminate, if the states $|f_k\rangle$ span the Hilbert space completely. In practice, this termination is only seen for very small systems, because the number of eigenstates grows exponentially with the size of the system.

A. Remarks on the numerical implementation

The sequence of coefficients a_k , b_k^2 have to be computed numerically. In order to give a rough estimate of the numerical effort required one should consider the maximum dimension D of the Hilbert space: The system considered contains $3N$ sites. N particles with spin up may be distributed on these sites in $\binom{3N}{N}$ possible ways, the remaining N spin-down particles may be located at the $2N$ unoccupied sites. Then the total dimension will be $(3N)!/(N!)^3$ which amounts to $\approx 10^{10}$ for $N = 8$.

In a first step, the ground state is constructed in terms of a basis with binary coding of the orbital occupation. For the implementation of the recursion it is essential to generate the ground state with maximum precision. Here, the ground state is known, e.g. we know an exact algorithm which generates the ground state by successive creation of particles out of the vacuum, according to Eq. (6). The coefficients of the ground-state basis elements are coded as integers. This eliminates all rounding errors.

The main part of the recursion Eqs. (12) is the implementation of the Hamilton operator. Whenever \bar{H} acts on a component of a state $|f\rangle$, $\bar{H}|f\rangle = |f'\rangle$, it is necessary to check whether the resulting basis components have already been generated before, in which case only amplitudes have to be added. Otherwise the newly generated basis components of $|f'\rangle$ have to be stored along with their amplitudes. This simple operation requires a large share of the numerical effort. In our algorithm this task is accelerated by application of binary trees. Then the overall numerical effort is of order $D \ln D'$, where D is the dimension of the input state $|f\rangle$ and D' the dimension of $|f'\rangle$. As stated above, D and D' increase exponentially with system size. By taking advantage of the symmetries mentioned above, a chain length of eight unit cells can be treated on a workstation with 128 Mbyte of computer memory. In

that case D is reduced to an amount of $\approx 10^6$ if symmetries are taken into account. Without explicit use of symmetries, $N = 6$ is the maximum system size.

VI. FINITE SIZE EFFECTS AND RECONSTRUCTION OF SPECTRAL DENSITIES

This section provides a brief recall how the information contained in the first continued-fraction coefficients can be reliably retrieved. Two problems need to be addressed: First, because of limited memory and CPU-power only finite systems can be studied, and, second, only a finite number of continued-fraction coefficients can be calculated.

The method applied here has been developed in the framework of an equivalent formulation (called Liouvillian representation) of the recursive algorithm outlined in Eqs. (12). This representation is based on an orthogonal expansion⁹ of the operator $A(t)$ and leads to a continued fraction of the form

$$\begin{aligned} c_0(z) &:= \int_0^\infty dt e^{-zt} \tilde{S}(t) \\ &= \frac{1}{z + \frac{\Delta_1}{z + \frac{\Delta_2}{z + \dots}}}. \end{aligned} \quad (16)$$

The functions $S(\omega)$ and $c_0(z)$ are connected by a Hilbert transform:

$$c_0(z) = \frac{1}{2\pi i} \int_{-\infty}^\infty d\omega \frac{S(\omega)}{\omega - iz} \quad (17)$$

$$S(\omega) = \lim_{\epsilon \rightarrow 0} 2 \Re[c_0(\epsilon - i\omega)] \quad (18)$$

The series of Δ_k can be uniquely obtained from the a_k - b_k^2 -series.

A. Finite size effects

Finite size effects can be eliminated by investigation of various data sets of Δ -coefficients with varying system size. The upper graph of Fig. 2 shows some data sets for chain lengths from four up to eight unit cells. The physical quantity under consideration is the spin

correlation function with $A = S_{q,\alpha=1}^z$. The data clearly illustrate that the finite size effects grow with increasing index k of Δ_k . Therefore it is essential to restrict the analysis to coefficients that are in good agreement with those corresponding to shorter systems and ignore the size dependent higher coefficients.

B. Termination

The full spectral information $S(\omega)$ is only accessible if all coefficients Δ_k (of an infinite system) are known. The question of how much information is contained in a finite Δ_k -series is by no means trivial and the goal of constructing a good approximation to the infinite continued fraction requires some care.

Let $\Gamma_K(z)$ be a terminator function that approximates the unknown rest of the continued fraction in “the best possible way”.

$$\bar{c}_0(z) = \cfrac{1}{z + \cfrac{\Delta_1}{z + \cfrac{\Delta_2}{z + \cfrac{\Delta_3}{\ddots + \cfrac{\Delta_{K-1}}{z + \Delta_K \Gamma_K(z)}}}} \quad (19)$$

The crudest approximation, $\Gamma_K(z) \equiv 0$, is equivalent to the “cut and smear out” procedure mentioned above. More adequate terminator functions may be obtained by analyzing the *implicit* information contained in the asymptotic behavior of the Δ_k -series.

In order to construct a more adequate terminator function, the pattern of Δ -coefficients for many generic situations have been analyzed in [13]; the corresponding terminator functions employed here are also discussed in [15]; the reader is referred to these sources for more technical information.

Generally, linear growth of Δ_k with k signals a Gaussian high-frequency decay of $S(\omega)$. Linear growth of both Δ_{2k} and Δ_{2k+1} with different slopes occurs if a spectral gap at low frequencies is present in $S(\omega)$. An example of this is shown in the lower panel of Fig. 2 [line a)]. Line b) in the same panel illustrates the characteristic change in the roles of even and

odd Δ 's when an additional zero-frequency peak is present in $S(\omega)$.

The size-independent numerically-calculated continued-fraction coefficients of the system under investigation show the generic patterns described above. Thus a model spectral function which corresponds to these patterns, $\bar{S}(\omega) = (2\sqrt{\pi}/\omega_0)\Theta(\omega - \omega_g)\exp\{-(\omega - \omega_g)^2/\omega_0^2\}$, is expanded into a model continued fraction. The gap-parameter ω_g and the width of the shifted half-Gaussian ω_0 are chosen such that the coefficients of the model continued fraction match the coefficients of the real system as close as possible. The terminator function $\Gamma_K(z)$ may be recursively obtained from the Hilbert transform of $\bar{S}(\omega)$.¹⁶

The spectral density is reconstructed using all size-independent coefficients calculated numerically and – instead of just truncating – extrapolating the asymptotic pattern to infinite order by “implanting” the customized terminator function. The more size independent explicitly known coefficients are taken, the less important are the details of the terminator. The main advantage of this termination procedure is the fact that a branch cut (in this formulation located on the imaginary axis of the complex plane) of $c_0(z)$ is *not* approximated by a finite set of isolated singularities; instead the function $\bar{c}_0(z)$ displays a branch cut itself.

The reconstruction of spectral densities is numerically performed by Eq. (18). The parameter ϵ is chosen as $\epsilon = 10^{-3}$. Reconstruction of the spectral densities with $\epsilon = 10^{-4}$ or $\epsilon = 10^{-5}$ yields results which coincide within the linewidth of Figs. 3-4.

VII. EXCITED STATES

The spectral densities obtained for spin- and charge degrees of freedom indicate that the excitation spectrum of the chain with $2N$ particles exhibits a gap or an energy region, where the spectral densities have very little weight. In order to gain complementary information on the excitation spectrum of the system under consideration, excited states and their corresponding eigenvalues have been calculated by an iterative algorithm often called conjugate-gradient method.^{17,18} If the starting vector overlaps with the ground state, the algorithm will iteratively determine the ground state. The same procedure will yield excited

states and excitation energies, if it is carried out in a subspace orthogonal to the ground state (provided the ground state is non-degenerate). Additionally, excited states are iteratively calculated in different symmetry subspaces. Fig. 5 provides the energy difference between the ground state and the lowest excited states as a function of system size.

VIII. RESULTS AND DISCUSSION

The present work investigates a Hubbard model of which the ground state and its energy can be calculated for a special number of particles $N_e = 2N$. This ground state has an RVB-structure. As far as the author knows, no other class of fermionic Hamiltonians with such a state being the exact ground state is known so far.

However, not many of the physical properties of this ground state and the excitations are known. Static correlation functions [the denominator in Eq. (11)] have been calculated for other one-dimensional representatives of this class⁴ by a transfer-matrix method. In all cases considered so far, the static correlation functions show an exponential decay.

The method presented above allows to calculate wave-vector dependent dynamical correlation functions making explicit use of the fact that the ground state is known. If the energy spectrum of the Hamiltonian has a gap, the spectral densities will show a gap as well. (The gap might be larger than the gap of the energy spectrum. In that case, this larger gap will be called *dynamical* gap.) The position of peaks in the reconstructed spectral densities as shown below reflect the dispersion relation $\omega_{peak}(q)$ of that particular excitation.

In order to corroborate the conclusions about a gap in the excitation spectrum, energies of the lowest excited states (without symmetry restriction) and those excited states that couple to the ground state are calculated.

Additionally, an attempt is made to gain information on the particle number regime below $N_e = 2N$ which has not been studied so far.

Fig. 3 shows spectral densities $S(\omega) = \int_{-\infty}^{\infty} dt \exp(i\omega t) \tilde{S}(t)$ [see Eq. (11)] for a spin degree of freedom $A = \sum_l \exp(iql)(n_{l,\alpha=1,\uparrow} - n_{l,\alpha=1,\downarrow})$ which measures the z -component of

the spin of the backbone electrons. All energies ω are given in units of the hopping matrix element (\hbar is set to unity). The translational symmetry is characterized by $q = 2\pi m/N$ with $m = 0 \dots N/2$. The data indicate that there is a (dynamical) gap in the spectrum. There is one dominating spin excitation present with q -independent energy (dispersionless). Both facts support the conjecture, that the system has an insulating⁴ ground state and that the properties are dominated by local effects. Only a very small spectral feature appears for $q \rightarrow \pi$ in the energy regime $\omega \approx 3$. All curves are normalized to π .

The operator $A = \sum_{l,\sigma} \exp(iql) n_{l,\alpha=1,\sigma}$ describes charge degrees of freedom of the backbone sites. The corresponding spectral density exhibits more than just one dominating excitation. For $q = 0$, the data in Fig. 4 show one very strong peak at $\omega = 0$. This simply reflects the $q = 0$ -symmetry of the ground state. For other q -values, features at higher energies appear. Their position does not change much with q , the corresponding excitations seem to be rather dispersionless.

The *dynamically relevant* gap is determined by the energy of the lowest excited state which couples via A to the ground state. Because the A -operators considered here commute with the singlet generator \mathbf{M}_s [see Eq. (8)], the lowest accessible excited state must have the symmetry $\mathbf{T}_q \mathbf{M}_s$ which is the symmetry of the state $A(q)|\Phi_0\rangle$. The data sets 2 and 3 in Fig. 5 show these excitation energies as a function of the system size. They seem to saturate at a constant level which indicates the existence of a dynamical gap. This conclusion is fully compatible to the reconstructed spectral data. However, the energies of the lowest excited states *without any restrictions on their symmetry* are located within the dynamical gap. Data set 1 provides these energies for chain lengths up to $N = 6$. A final judgement, whether these energies saturate or not cannot be made, because larger systems cannot be treated without taking advantage of symmetries.

Further, the variationally calculated energies show only very little dependency on the wave vector q which confirms the very small shift of the peak in Fig. 3.

The recursion method is not restricted to hermitean operators A only. Fig. 6 provides

results for $A = \sum_l \exp(iql) c_{l,\alpha=1,\sigma}$ which annihilates backbone electrons in a translationally invariant way. Then the quantity $\tilde{S}(t)$ of Eq. (11) becomes a single-hole propagator. Its Fourier transform may be related to inverse photoemission spectra.

Characteristic features of the single-hole spectral function shown in Fig. 6 are a broad continuum of states and a q -dependent gap. Unfortunately the origin of the ω -axis is not known, because the smallest eigenvalue λ of the Hamiltonian $\bar{H} = H + 4N + 2$ cannot be calculated. The single-hole states are delocalized (i. e. show dispersion) and may contribute to electronic conduction.

ACKNOWLEDGMENTS

The author is indebted to J. Stolze who generously shared his experience and knowledge about continued fractions and their termination. His “toolbox” allowed to reconstruct the spectral densities efficiently and has been of valuable help. J. Richter was so kind to provide some of his computer power during software development. The author gratefully acknowledges many helpful discussions with W. Wenzel, H. Keiter and U. Brandt. This work has been supported by the Deutsche Forschungsgemeinschaft (DFG), Project Br 434/6-2.

REFERENCES

¹ J. Hubbard, Proc. R. Soc. London Ser. A **276**, 238 (1963); M. C. Gutzwiller, Phys. Rev. Lett. **10**, 159 (1963); J. Kanamori, Prog. Theor. Phys. **30**, 275 (1963).

² U. Brandt and A. Gieseckus, Phys. Rev. Lett. **68**, 2648 (1992).

³ R. Strack, Phys. Rev. Lett. **70**, 833 (1993); R. Strack and D. Vollhardt Phys. Rev. Lett. **70**, 2637 (1993).

⁴ P.-A. Bares and P. A. Lee Phys. Rev. B **49**, 8882 (1994).

⁵ H. Tasaki, Phys. Rev. Lett. **70**, 3303 (1993).

⁶ H. Tasaki, Phys. Rev. B. **49**, 7763 (1994).

⁷ L. Pauling, Proc. R. Soc. London A **196**, 343 (1949); P. W. Anderson, Mater. Res. Bull. **8**, 153 (1973); P. Fazekas and P. W. Anderson, Philos. Mag. **30**, 423 (1974).

⁸ R. Haydock, Solid State Phys. **35**, 215 (1980).

⁹ M. H. Lee, Phys. Rev. B **26**, 2547 (1982).

¹⁰ E. R. Gagliano, E. Dagotto, A. Moreo, and F. C. Alcaraz Phys. Rev. B **34**, 1677 (1986).

¹¹ V. S. Viswanath and G. Müller, J. Appl. Phys. **67**, 5486 (1990).

¹² *The recursion method and its applications*, edited by D. G. Pettifor and D. L. Weaire (Springer-Verlag, New York, 1985).

¹³ V. S. Viswanath and G. Müller, *The Recursion Method – Application to Many-Body Dynamics*, Springer-Verlag Berlin Heidelberg (1994).

¹⁴ C. Lanczos, J. Res. Nat. Bur. Stand. **45**, 255 (1950).

¹⁵ V. S. Viswanath, S. Zhang, J. Stolze, and G. Müller Phys. Rev. B **49**, 9702 (1994).

¹⁶ The corresponding integral [see Eq. (17)] leads to a sum of the complex error function and

the complex exponential integral.

¹⁷ W. W. Bradbury and A. Fletcher, *Num. Math.* **9**, 259 (1966).

¹⁸ M. P. Nightingale, V. S. Viswanath, and G. Müller, *Phys. Rev. B* **48**, 7696 (1993).

FIGURES

FIG. 1. Two illustrations of the Hubbard chain: a) The filled circles denote the sites, the solid lines indicate the bonds, where hopping is possible. The dashed line frames one unit cell. Sites within a unit cell are labeled by an index $\alpha = 1, 2, 3$. b) The topology of the chain may also be visualized by a chain of connected tetrahedra.

FIG. 2. Continued-fraction coefficients Δ_k verus k . The upper graph shows coefficients obtained for the $q = 0$ spin degree of freedom $A = \sum_l S_{l,\alpha=1}^z$ for various system sizes $N = 4 - 8$ with particle numbers of $2N$. The lower graph shows two generic patterns of coefficients. Data a) are identical to the spin data for 8 unit cells of the upper graph. The set b) displays results for the $q = 0$ charge degree of freedom $A = \sum_{l,\sigma} n_{l,1,\sigma}$. Lines are intended to guide the eye.

FIG. 3. Reconstructed spectral densities (Gaussian terminator, $\epsilon = 10^{-3}$) for spin degrees of freedom $A_q = \sum_l \exp\{iql\} S_{l,\alpha=1}^z$. The first 16 continued-fraction coefficients calculated for the chain with $N = 8$ were taken into account.

FIG. 4. Reconstructed spectral densities (Gaussian terminator [with gap for $q > 0$], $\epsilon = 10^{-3}$) for charge degrees of freedom $A_q = \sum_{l,\sigma} \exp\{iql\} n_{l,\alpha=1,\sigma}$. The first 16 continued-fraction coefficients calculated for the chain with $N = 8$ were taken into account.

FIG. 5. Energy differences $E - E_0$ between excited-state eigenvalues and the ground-state energy for systems with N unit cells and $2N$ particles. Data set 1 provides results without any symmetry restrictions, results in set 2 (set 3) are based on the assumption that the corresponding excited state $|\Psi\rangle$ has the symmetry $\mathbf{T}_{q=0}\mathbf{M}_s|\bar{\Psi}\rangle$ ($\mathbf{T}_{q=\pi}\mathbf{M}_s|\bar{\Psi}\rangle$). Lines are intended to guide the eye.

FIG. 6. Reconstructed spectral densities (Gaussian terminator with gap, $\epsilon = 10^{-3}$) for the hole propagator $A_q = \sum_l \exp\{iql\} c_{l,\alpha=1,\sigma}$. The first 16 continued-fraction coefficients calculated for the chain with $N = 8$ were taken into account. The origin of the ω -axis is shifted by the unknown smallest eigenvalue λ of \bar{H} for $N_e = 2N - 1$

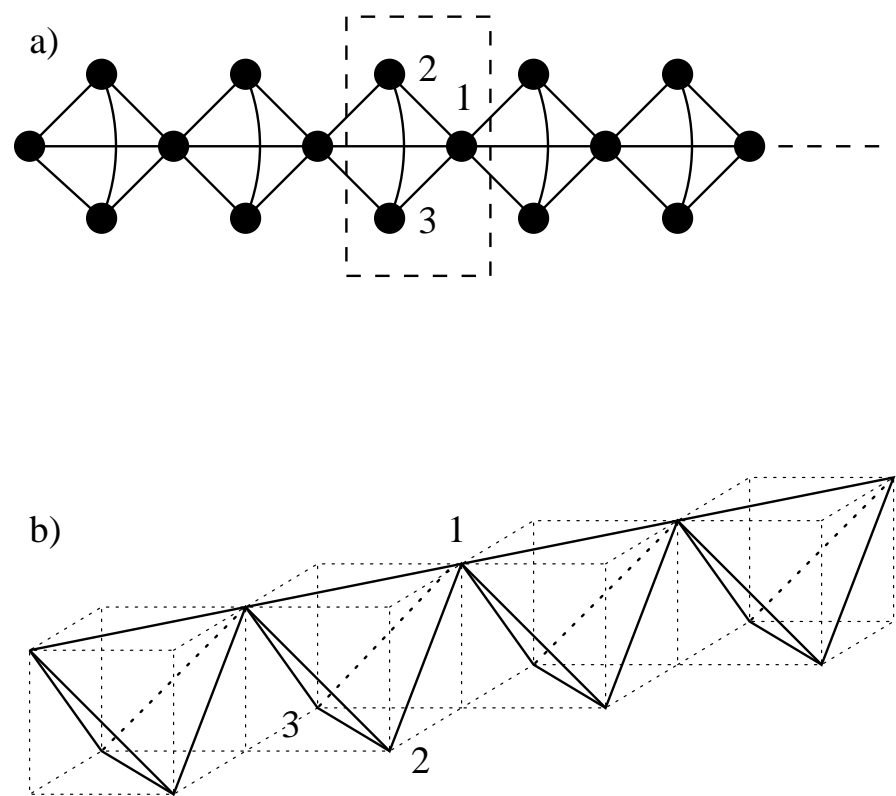


Figure 1

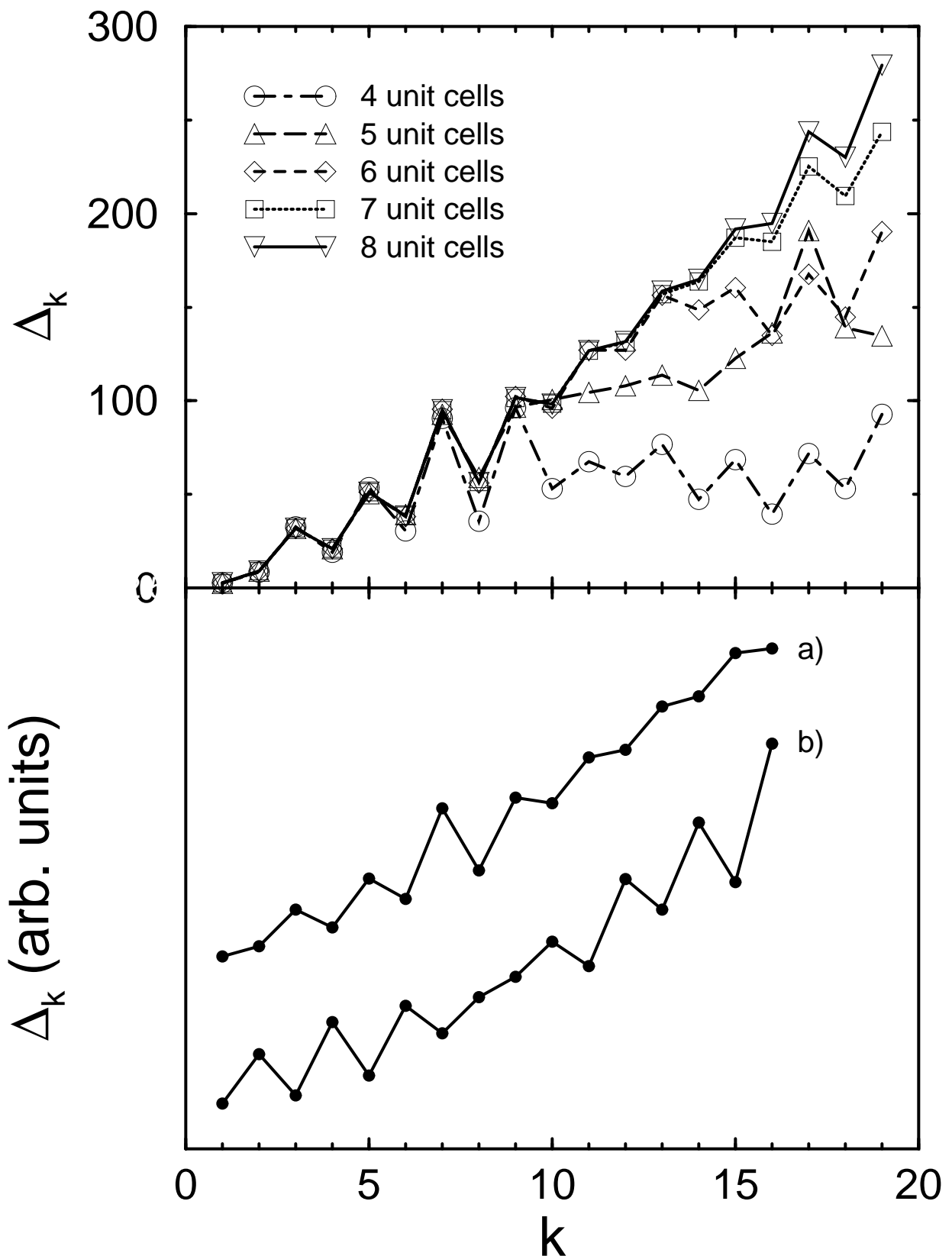


Figure 2

Figure 3

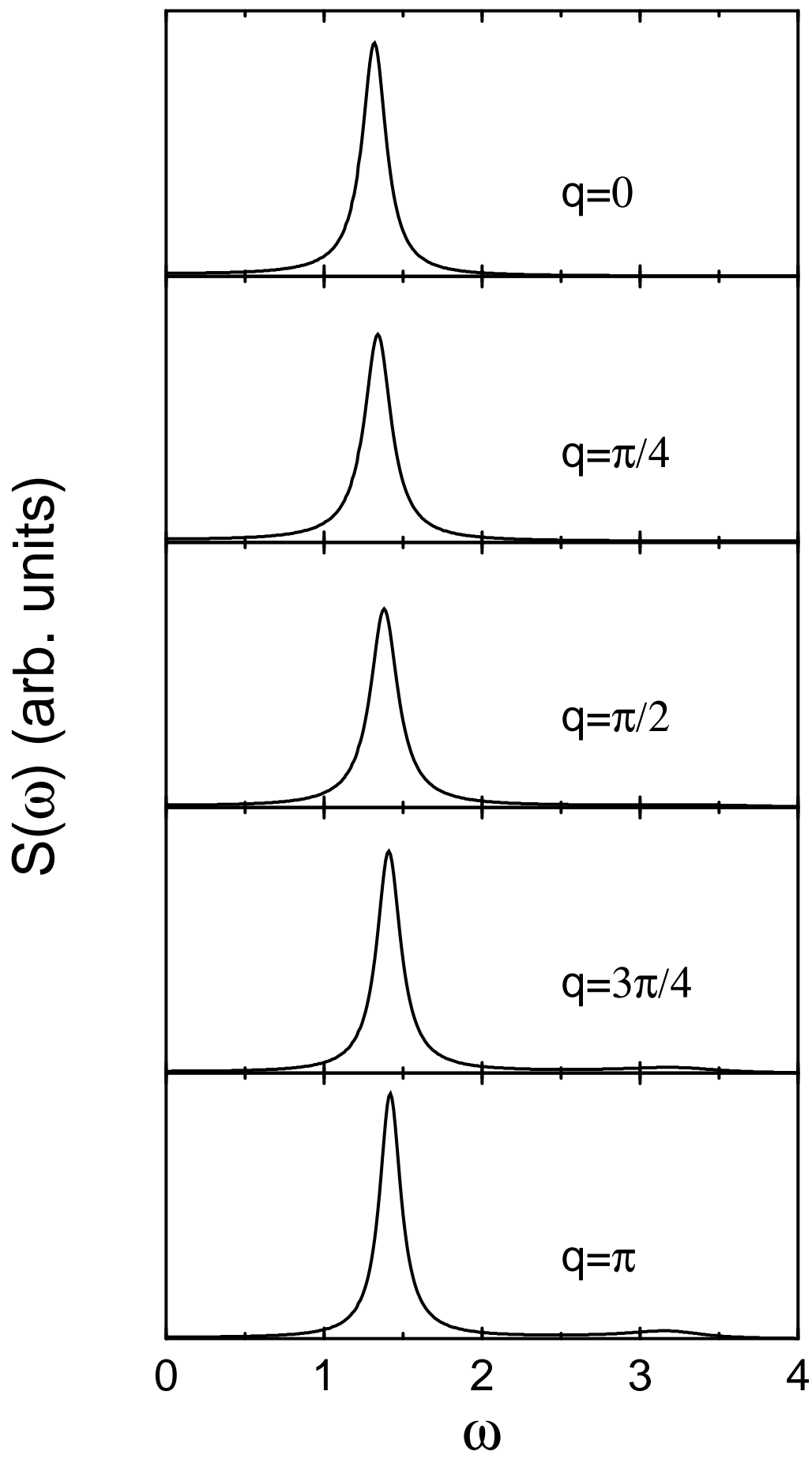


Figure 4

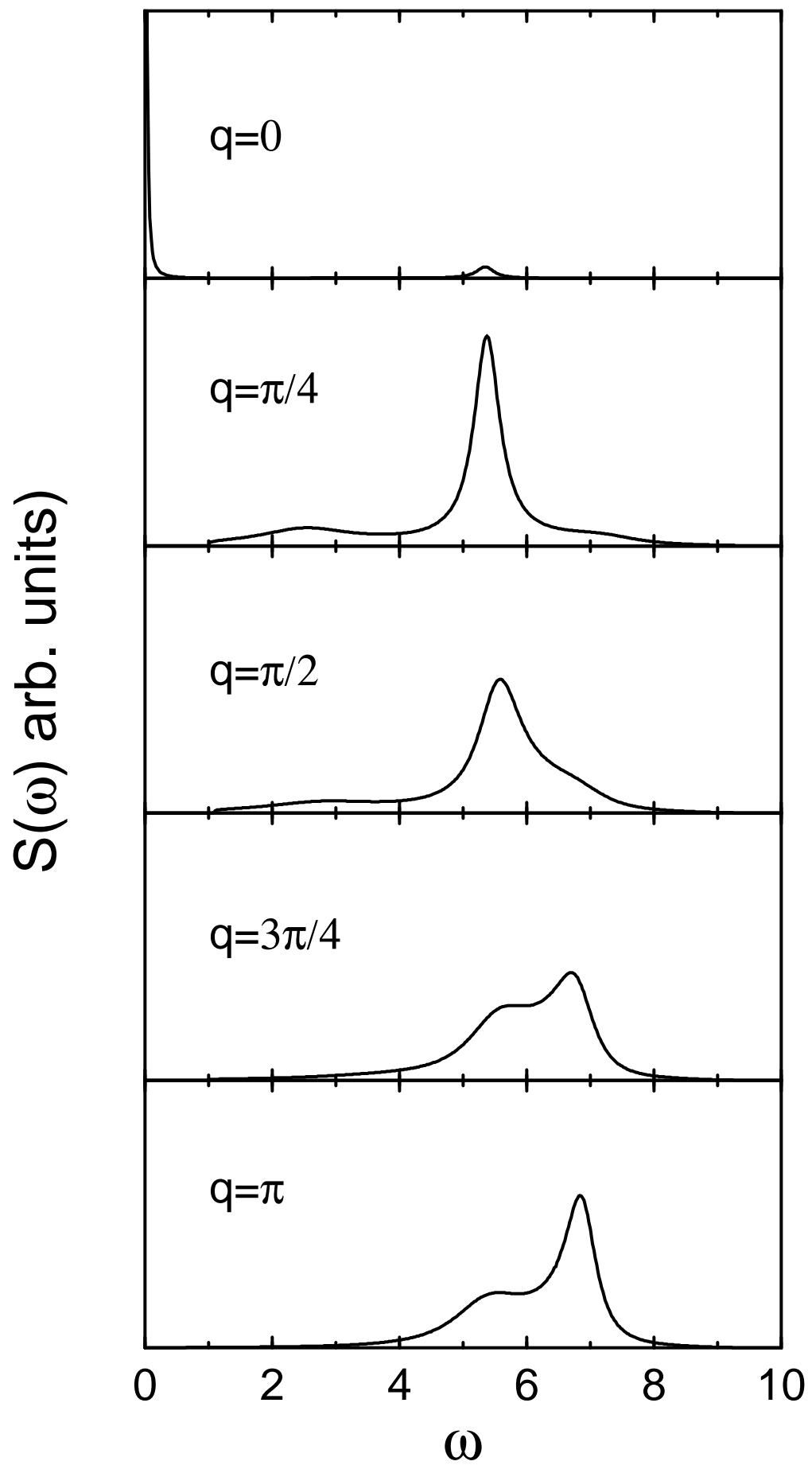


Figure 5

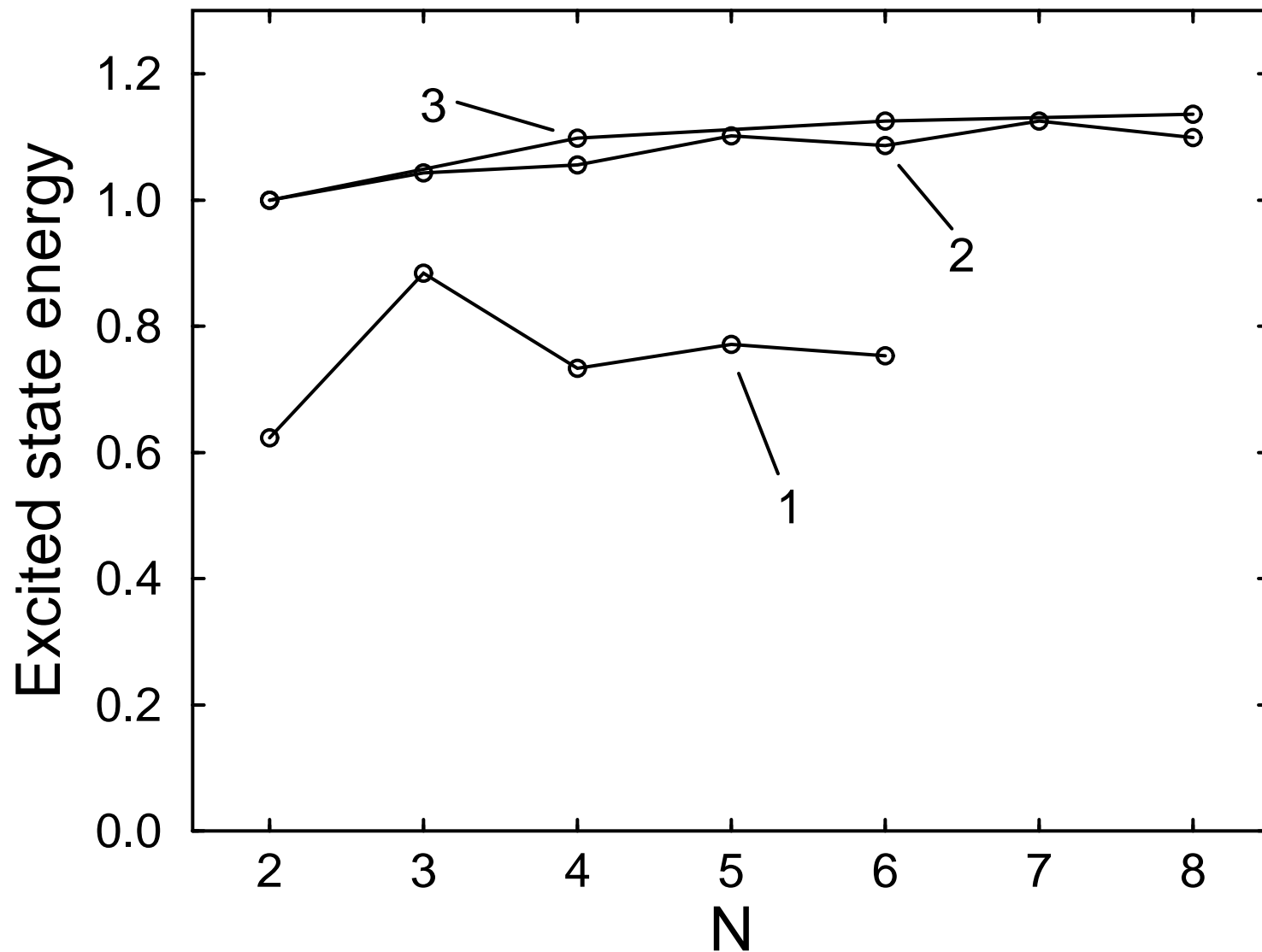


Figure 6

